Available online at www.sciencedirect.com
ScienceDirect
Tetrahedron: Asymmetry
Tetrahedron: *Asymmetry* 17 (2006) 2504–2510

Highly efficient NMR enantiodiscrimination of 1,1,1,3,3-pentafluoro-2-(fluoromethoxy)-3-methoxypropane, a chiral degradation product of sevoflurane, by heptakis(2,3-di-*O*-acetyl-6-*O*-*tert*-butyldimethylsilyl)-β-cyclodextrin

Gloria Uccello-Barretta,[a] Giuseppe Sicoli,[b] Federica Balzano,[a] Volker Schurig[b] and Piero Salvadori[a,*]

[a] *Università degli Studi di Pisa, Dipartimento di Chimica e Chimica Industriale, Via Risorgimento 35, I-56126 Pisa, Italy*
[b] *Universität Tübingen, Institut für Organische Chemie, Auf der Morgenstelle 18, D-72076 Tübingen, Germany*

Received 31 July 2006; accepted 18 September 2006

Abstract—The molecular basis of the efficient enantiodiscrimination of 1,1,1,3,3-pentafluoro-2-(fluoromethoxy)-3-methoxypropane, a chiral degradation product of the inhalation anaesthetic sevoflurane, using heptakis(2,3-di-*O*-acetyl-6-*O*-*tert*-butyldimethylsilyl)-β-cyclodextrin as chiral selector, has been investigated by NMR spectroscopy. An interaction mechanism is proposed, which highlights the role of the functional groups on the β-cyclodextrin rims in addition to a partial molecular inclusion.

1. Introduction

Achiral sevoflurane represents a fluorinated derivative of methyl isopropyl ether, which has been under development since 1992 for use as a human inhalation anaesthetic.[1–5] It provides fast, irritation-free inhalation induction and rapid recovery. Upon anaesthesia, sevoflurane is recycled in a re-breathing unit containing soda lime to absorb exhaled carbon dioxide, accompanied by minor chemical transformations. Among the degradation products,[6] the chiral fluorinated diether, racemic 1,1,1,3,3-pentafluoro-2-(fluoromethoxy)-3-methoxypropane **1** (Fig. 1) was identified.

By using enantioselective GC, some cyclodextrin derivatives exhibited unprecedented high separation factors α for **1**.[7–10] Thus, heptakis(2,3-di-*O*-acetyl-6-*O*-*tert*-butyldimethylsilyl)-β-cyclodextrin **2** (Fig. 1), dissolved in PS 86 (20% w/w), could be used for the isolation of pure enantiomers of **1** by preparative GC.[7]

With the aim of exploring the origin of chiral recognition processes, we employed **2** as a chiral solvating agent (CSA)[11–14] for inducing NMR anisochrony of the exter-

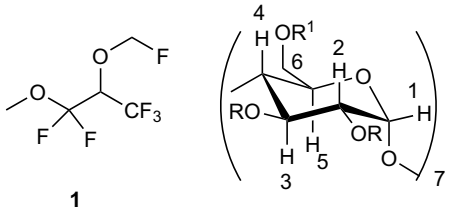

Figure 1. Structures of compound **1** and silylated/acetylated cyclodextrin derivative **2**.

nally enantiotopic nuclei of **1** and exploited several NMR methods, including DOSY (Diffusion-Ordered SpectroscopY) techniques,[15] to investigate the geometry, dynamics and thermodynamics of the diastereomeric complexes formed by **2** and the single enantiomers of **1** in solution.

2. Results and discussion

2.1. Enantiodiscrimination experiments

The mixed silylated/acetylated cyclodextrin **2** was synthesized according to the procedure of Takeo et al.[16] For

* Corresponding author. Tel.: +39 0502219203; fax: +39 0502219409; e-mail: psalva@dcci.unipi.it

0957-4166/$ - see front matter © 2006 Elsevier Ltd. All rights reserved.
doi:10.1016/j.tetasy.2006.09.019

the gas-chromatographic analysis, deactivated silica capillaries were coated by the static method[17] with 20% (w/w) **2** dissolved in the polysiloxane PS 086 (12–15% diphenyl; 85–88% dimethyl). The remarkably high enantioseparation factor of $\alpha = 4.1$ found between **1** and **2**[7] prompted us to investigate the enantiodiscrimination processes in solution by NMR spectroscopy employing selector **2** as a chiral solvating agent. If the enantiomers of **1** form transient diastereomeric association complexes with CSA **2**, chemical shift non-equivalence ($\Delta\delta = |\delta_S - \delta_R|$) may arise due to (i) different association constants K_S and K_R and/or (ii) distinct geometries of the formed diastereomers,[11] whereby the two independent contribution to anisochrony are difficult to separate (vide infra).

To this end, the ^{1}H and ^{19}F NMR spectra of **1** (20 mM) in the presence and in the absence of **2** (20 mM) were compared with each other. The nature of the solvent employed in the NMR experiments plays a fundamental role: in chloroform or dichloromethane solution, anisochrony of racemic **1** was not observed in the presence of **2**. In an apolar deuterated cyclohexane solution the β-cyclodextrin derivative **2** produced surprisingly high proton chemical shift non-equivalences for racemic **1**, confirming the remarkable efficiency of **2** as chiral selector for its enantiodiscrimination.

Thus the methoxy protons of racemic **1** exhibited two sharp singlets at 3.59 and 3.61 ppm (Fig. 2b and Table 1).

The anisochrony measured for the methine resonances (Fig. 2f) was much larger (0.074 ppm). The methylene protons were also differentiated, but the signals were partially superimposed by the proton resonances of the CSA **2**. In the next step, the proton resonances of the isolated single (*R*)- and (*S*)-enantiomers of **1**, obtained by preparative GC,[7] were detected in the presence of **2**. It was established that (*S*)-**1** shows larger complexation shifts (differences between the chemical shifts of corresponding nuclei of **1** in the presence and in the absence of the chiral auxiliary **2**) compared to (*R*)-**1** (Fig. 2). This observation is in agreement with the GC experiment whereby (*S*)-**1** is eluted after the (*R*)-enantiomer on the selector **2**.[7] Interestingly all of the resonances of (*S*)-**1** are higher frequency shifted relatively to (*R*)-**1**. A further increase in the chemical shift non-equivalences could be obtained by increasing the equimolar concentration of **1** and **2** (Fig. 2d and h and Table 1), by adding further equivalents of the CSA **2** (Fig. 2c and g and Table 1) and by lowering the temperature (Table 1), leading to non-equivalences till to 0.18 ppm. It is noteworthy that by lowering the temperature to 10 °C it gives non-equivalences increases comparable to the ones obtained by a threefold increase of the total concentration.

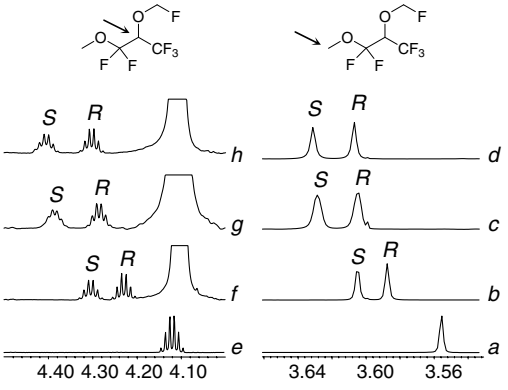

Figure 2. ^{1}H NMR (600 MHz, C_6D_{12}, 25 °C) spectral regions corresponding to the protons of the CH_3O-group of (a) pure racemic **1** (20 mM), (b) equimolar mixture of racemic **1** and **2** (20 mM), (c) racemic **1** (20 mM) and **2** (40 mM), (d) equimolar mixture of racemic **1** and **2** (60 mM). ^{1}H NMR (600 MHz, C_6D_{12}, 25 °C) spectral regions corresponding to the protons of the CH-group of (e) pure racemic **1** (20 mM), (f) equimolar mixture of racemic **1** and **2** (20 mM), (g) racemic **1** (20 mM) and **2** (40 mM), (h) equimolar mixture of racemic **1** and **2** (60 mM).

Table 1. ^{1}H NMR (600 MHz, C_6D_{12}) chemical shift non-equivalence[a] data measured for racemic **1** in the presence of **2**

	(*RS*)-**1**/**2** (1:1)				(*RS*)-**1**/**2** (1:2)	
	20 mM		60 mM		20 mM	
	25 °C	10 °C	25 °C	10 °C	25 °C	10 °C
CH	0.074	0.142	0.111	0.176	0.105	0.171
OCH_3	0.020	0.032	0.026	0.041	0.024	0.039

[a] $|\delta_S - \delta_R|$, difference between the chemical shifts (ppm) of corresponding nuclei of the two enantiomers of **1** in the presence of **2**.

Anisochrony induced in the ^{19}F nuclei (Table 2) was remarkably high: it ranged from 0.21 to 0.52 ppm for the 20 mM equimolar mixture of **1** and **2**. It significantly increased for the 60 mM equimolar mixture (0.30–0.72 ppm) and for the 20 mM solution added by another equivalent of **2** (0.25–0.73 ppm).

Table 2. ^{19}F NMR (282 MHz, C_6D_{12}, 25 °C) chemical shift non-equivalence[a] data measured for racemic **1** in the presence of **2**

	20 mM		60 mM
	1:1	1:2	1:1
CF_3	0.206	0.249	0.303
CF_2	0.363	0.514	0.520
	0.521	0.727	0.722
CH_2F	0.422	0.487	0.571

[a] $|\delta_S - \delta_R|$, difference between the chemical shifts (ppm) of corresponding nuclei of the two enantiomers of **1** in the presence of **2**.

As in the case of proton nuclei, fluorine resonances of the two enantiomers were higher frequency shifted compared with pure **1** and (*S*)-**1** exhibits larger complexation shifts than (*R*)-**1** does in agreement with the GC experiment.

2.2. Association constants

The 1:1 stoichiometric ratios between the components of the diastereoisomeric complexes (*R*)-**1** and **2** and (*S*)-**1** and **2** formed in solution were established by Job's method.[18,19]

For the determination of the association constants, DOSY measurements[15] were taken into consideration, which constitute a fast and efficient alternative to the well-established chemical shift titrations,[20] at least in the cases of inclusion complexes.

DOSY techniques make it possible to measure diffusion coefficients (D) in solution. For spherical particles of hydrodynamic radius R_H in a solvent of viscosity η, the diffusion coefficients are given by Eq. 1

$$D = \frac{kT}{6\pi\eta R_H} \quad (1)$$

where k is the Boltzmann constant and T is the temperature.

Therefore diffusion coefficients represent global parameters, which are characteristic of molecular species as a whole. In this respect these parameters have great potential in the detection of complexed species, in which an increase of molecular sizes, and hence a decrease of diffusion coefficients with respect to uncomplexed forms, should be expected. Despite the fact that the molecular sizes of two diastereoisomeric solvates are similar in principle, DOSY techniques can also be used in the analysis of enantiodiscrimination phenomena. Under the rapid exchange conditions occurring in solutions containing mixtures of complexing species, measured diffusion coefficients D_{obs} are the weighted average of their values in free (D_f) and bound (D_b) states

$$D_{obs} = X_b D_b + (1 - X_b) D_f \quad (2)$$

Thus the two complexed enantiomers can be differentiated on the basis of their different bound fractions. Even more importantly, in the cases of cyclodextrin inclusion complexes, D_b is very likely to be equal to that of the cyclodextrin since the guest molecule is small compared to the host molecule; and therefore, global diffusion can be assumed to be controlled by the host.[21] Therefore Eq. 3 can be used to calculate the molar fractions of the two bound enantiomers (X_b)

$$X_b = \frac{D_{obs} - D_f}{D_b - D_f} \quad (3)$$

where $D_b = D_{cyclodextrin}$ and the association constant can be calculated by substituting the X_b values to the following K equation (for a 1:1 complex)

$$K = \frac{X_b}{C_0(1 - X_b)^2} \quad (4)$$

where C_0 is the known concentration of the selector and the analyte.

On the basis of the above approach, we compared the DOSY maps of the pure compounds **1** and **2** (60 mM, C_6D_{12}) with those of the equimolar mixtures **2**/(*R*)-**1** and **2**/(*S*)-**1** (Table 3). For the pure cyclodextrin we measured a diffusion coefficient of 1.28×10^{-10} m^2 s^{-1}, which did not change in the two mixtures **2**/(*R*)-**1** and **2**/(*S*)-**1**. By contrast, the diffusion parameter of the fluorinated diether decreased from 13.4×10^{-10} m^2 s^{-1} in pure **1** to 6.67×10^{-10} m^2 s^{-1} for **2**/(*R*)-**1** and 5.94×10^{-10} m^2 s^{-1} for **2**/(*S*)-**1**. Thus, by using Eq. 3, the values of bound fractions obtained were 0.56 and 0.62 for (*R*)-**1** and (*S*)-**1**, respectively, leading to obtain, by a single point determination, the two association constants of the two 1:1 diastereoisomeric solvates as $K_R = 48.2$ M^{-1} and $K_S = 71.6$ M^{-1} (Table 3).

Table 3. Diffusion coefficients D (10^{-10} m^2 s^{-1}) of **1** and **2**; molar fraction of the bound guest (X_b) and association constants K (M^{-1}) calculated according to Eq. 4

	D (10^{-10} m^2 s^{-1})	X_b	K (M^{-1})
1	13.4		
2	1.28		
(*R*)-**1**/**2**	6.67	0.56	48.2
(*S*)-**1**/**2**	5.94	0.62	71.6

Reliability of the above approach was verified by using the same procedure to calculate the association constants of the two diastereoisomeric solvates in solutions containing a fixed amount (2 mM) of (*S*)- and (*R*)-**1** and increasing quantities of **2** (2–30 mM), that is, in experiments that mimic the chromatographic conditions with the excess of cyclodextrin as CSP.

2.3. Conformational analysis of the chiral selector 2

Before analyzing the stereochemical features of the diastereomeric complexes formed between (*R*)-**1** or (*S*)-**1** and **2**, conformation of pure **2** was analyzed in order to detect expected modifications on the structure of the native β-cyclodextrin after derivatization, which could affect its complexing properties.

The rotation of glucopyranose units about the glycosidic linkages and deviations of the glucopyranose rings from the common $^4C_1$ chair conformation was ascertained via an accurate analysis of intra- and interunit interproton dipolar interactions detected in the ROESY map (C_6D_{12}, 25 °C, mix 0.3 s), successfully applied previously to other kinds of cyclodextrin derivatives.[22–24]

Above analysis protocol is mainly based on the comparison of relative intensities of H-1–H-4′ (the apex indicates protons belonging to the unit adjacent to the one taken into consideration) and H-1–H-2 dipolar interactions, which reflect the extent of the rotation of glucopyranose units about the glycosidic linkages, and on the detection of unexpected 1,2-diaxial effects, at the expenses of expected 1,3-diaxial ones, which are diagnostic of distortions occurring in the chair conformation. In fact the C–H-1 and C–H-4′ bonds of native cyclodextrins are held coplanar by the strong network of attractive hydrogen bonding interactions between secondary hydroxyl groups, which renders the distance H-1–H-4′ significantly shorter with respect to that of H-1–H-2. In these cases, the dipolar interaction H-1–H-4′ is more intense than the H-1–H-2 is. The intensities of the ROEs H-1–H-4′ and H-1–H-2 of **2** (Fig. 3b) were comparable, which reflects the lengthening of the interunit H-1–H-4′ distance with respect to the fixed intraunit H-1–H-2 one, caused by the rotation about glycosidic linkages. The clockwise and anticlockwise rotations of the units alternatively bring the proton H-1 of one unit in proximity to the internal protons H-3′ and H-5′ of adjacent ones and in the trace of the proton H-1 the corresponding ROEs were detected (Fig. 3b).

As far as glucopyranose rings distortions are concerned, in the trace of the proton H-2 (Fig. 3c) not only the ex-

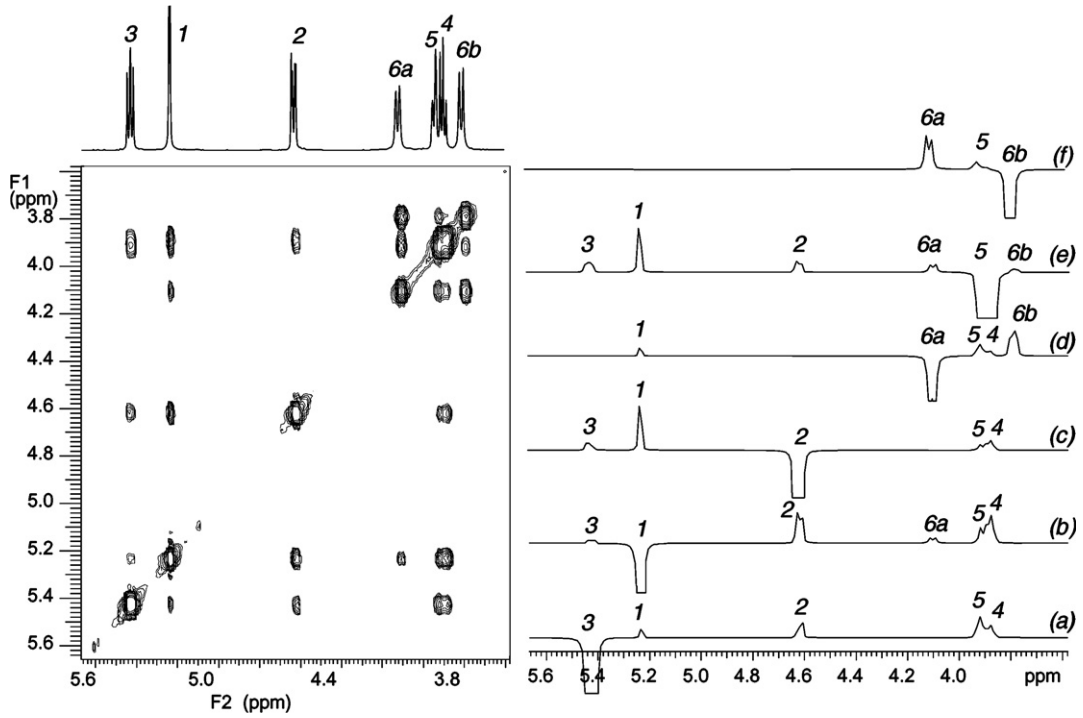

Figure 3. 2D ROESY (600 MHz, C_6D_{12}, 25 °C, $\tau_m = 0.3$ s) map of **2**. Traces corresponding to the (a) H-3, (b) H-1, (c) H-2, (d) H-6a, (e) H-5 and H-4 and (f) H-6b protons.

pected 1,2-axial–equatorial and 1,3-diaxial dipolar interactions with the H-1 and H-4 protons were detected, respectively, but also a ROE with the internal proton H-3, which should be 1,2-diaxial with respect to it. Interestingly, interROEs H-2–H-4 and H-2–H-3 not only were comparable to each other, but also were both smaller with respect to the H-2–H-1 effect. Taking into account that, in the fast exchange conditions, the observed effects are the average on all the glucopyranose rings, it can be concluded that some chair distortions bring the protons H-2 and H-3 closer and lengthen the H-2–H-4 distances with respect to the H-2–H-1 ones. Therefore, as previously reported for persubstituted cyclodextrins,[22–24] a significant population of *skew* conformers (Fig. 4, $^{O}S_5$) must be present having the H-3, H-2 and H-4 protons inverted to the equatorial positions. Accordingly, proton H-3 (Fig. 3a) gave unexpected dipolar interactions with the protons H-2 and H-4. Other dipolar interactions support the above conclusion. In the *skew* conformers, the 2-acetyl groups residing in an axial position are close to the proton H-5 (Fig. 4) and the corresponding dipolar interaction, although weak, was clearly detected in the trace of the acetyl groups.

Both conformational changes, that is, relative rotation and distortion, were confirmed by the interROEs between the 6-$(CH_3)_3$C- or 6-$(CH_3)_2$Si-fragments and the 2- and 3-acetyl groups (Fig. 4).

The above analysis is in agreement with the values of the average interproton distances (Table 4), calculated from the cross-relaxation rates σ_{ij}, which, in the initial rate approximation,[25] are a simple function of the reorientational correlation time τ_c of the vector connecting the two protons i and j and of their interproton distance r_{ij}:

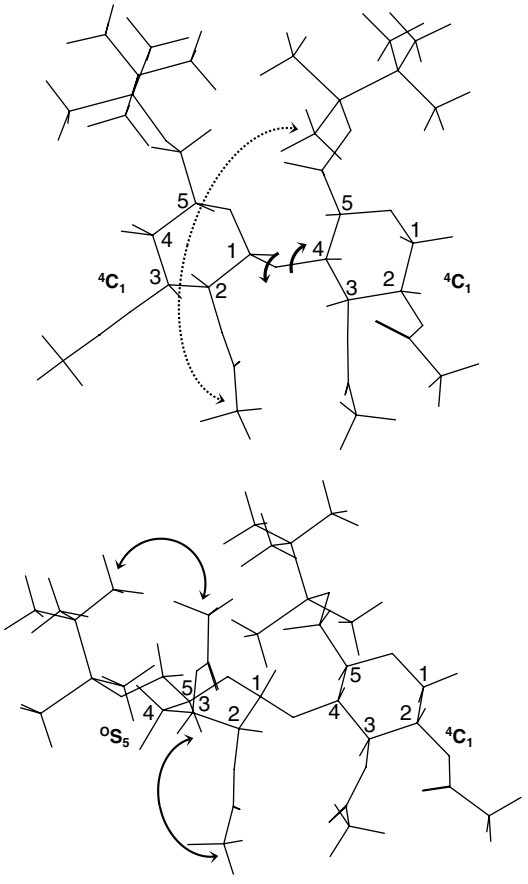

Figure 4. Schematic representation of a $^4C_1$ glucopyranose unit of **2** adjacent to another $^4C_1$ unit and adjacent to a skew unit.

Table 4. Measured mono- (R_i^{ms}, s^{-1}), biselective (R_{ij}^{bs}, s^{-1}) and cross-relaxation (σ_{ij}, s^{-1}) rates for the protons of **2** (60 mM, C_6D_{12}, 25 °C) and calculated interproton distances (r_{ij}, Å)

ij	R_i^{ms} (s^{-1})	R_{ij}^{bs} (s^{-1})	σ_{ij} (s^{-1})	r_{ij} (Å)
6a6b	3.26	1.73	−1.53	1.78[27]
12	1.60	1.22	−0.38	2.25
14'	1.60	1.19	−0.41	2.21
23	1.13	0.85	−0.28	2.62
34	0.95	0.76	−0.19	2.51

$$\sigma_{ij} = 0.1\gamma^4\hbar^2 r_{ij}^{-6}\tau_c\left[\frac{6}{1+4\omega^2\tau_c^2} - 1\right] \quad (5)$$

where γ is the proton gyromagnetic ratio, ω is the proton Larmor frequency and $\hbar$ is the reduced Planck's constant. In the fast and slow motion regimes ($\omega^2\tau_c^2 \ll 1$ and $\omega^2\tau_c^2 \gg 1$, respectively) the above equation can be approximated as

$$\text{fast motion } \sigma_{ij} = 0.5\gamma^4\hbar^2 r_{ij}^{-6}\tau_c \quad (6)$$

$$\text{slow motion } \sigma_{ij} = -0.1\gamma^4\hbar^2 r_{ij}^{-6}\tau_c \quad (7)$$

Such parameters σ_{ij} can be very simply obtained as the difference between the biselective (R_{ij}^{bs}) and monoselective (R_i^{ms}) relaxation rates,[26] respectively, measured by simultaneously inverting the spins *i* and *j* and selectively inverting the spin *i* alone, and hence following the recovery of magnetization of *i*.

In the hypothesis of isotropic motion, the ratios of the cross-relaxation terms are very simply correlated to the ratios of the interproton distances

$$\frac{\sigma_{ij}}{\sigma_{ik}} = \frac{r_{ik}^6}{r_{ij}^6} \quad (8)$$

On the basis of Eq. 8, the interproton distances between spins *ij* can be determined being fixed and known the distance between another proton pair *ik*.

Thus, the monoselective relaxation rate of the proton H_{6a} or H_{6b} (R_{6a}^{ms}) of **2** and their respective biselective relaxation rates (R_{6a6b}^{bs}), which are listed in Table 4, were measured. From their differences the cross-relaxation parameter (σ_{6a6b}), corresponding to the fixed interproton distance of 1.78 Å,[27] was calculated. It should be noted that the cross-relaxation rate was negative, reflecting the slowing down of the molecular motion of the cyclodextrin due to the introduction of three groups on every unit.

In the same way the σ_{ij} cross-relaxation terms of selected proton pairs collected in Table 4 were calculated and, hence, by Eq. 8, the average interproton distances r_{ij} were determined (Table 4).

The distance r_{12} of 2.25 Å corresponded to the average value for two protons in an axial-equatorial spatial relationship, but its similarity to the distance H-1–H-4′ (2.21 Å) reflected the tilting of the glucopyranose rings. Furthermore, the distances r_{23} (2.62 Å) and r_{34} (2.51 Å) were too short to be attributed to their 1,2-diaxial positions in the $^4C_1$ chair conformation, according to the fact that derivatization generated a distortion that made shorter above distances than they were in the $^4C_1$ chair unit conformers.

2.4. Geometry of the association complexes (*S*)-1/2 and (*R*)-1/2

In order to obtain information on the geometry of the diastereomeric association complexes in solution, the 2D and 1D ROESY spectra of 60 mM equimolar solutions (*S*)-**1/2** and (*R*)-**1/2** (C_6D_{12}, 25 °C) were analyzed. The above concentration value guaranteed the formation of detectable amounts of bound species. The pattern of intramolecular ROEs for **2** demonstrated that the conformation of the cyclodextrin did not change after the complexation with (*R*)- or (*S*)-**1**. Also the conformation of **1** remained unchanged because for the analyte the intramolecular ROEs detected for the free and bound states were also the same.

In both diastereomeric association complexes, the CH_3O-group of the fluorinated diether **1** is far away from the CH_2F group, whereas the CH-group is directed towards it. In fact, only the proton on the stereogenic centre produced significant dipolar interaction with the CH_2F group (Fig. 5a and b are referred to (*R*)-**1/2** mixture).

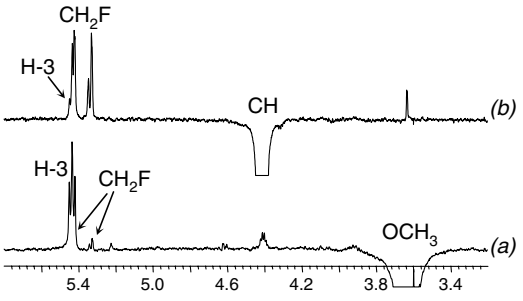

Figure 5. 1D ROESY (600 MHz, C_6D_{12}, 25 °C, $\tau_m = 0.3$ s) spectra of equimolar mixtures (*R*)-**1/2** (60 mM) corresponding to (a) CH_3O-protons and (b) CH-proton of **1**.

As far as the intermolecular ROEs are concerned, for both enantiomers of **1** the CH_3O-group of **1** produced a very intense dipolar interaction with the inner H-3 proton (Fig. 5a) lying on the wider internal diameter part of the cavity of cyclodextrin **2**.

No relevant intermolecular dipolar interactions were detected between the CH_3O-group and the inner H-5 proton belonging to the narrower internal diameter part of the cavity. The CH-proton adjacent to the CH_3O-group produced significantly lower ROE on the H-3 proton (Fig. 5b), which suggests that both enantiomers of **1** undergo inclusion into the cyclodextrin derivative **2** only by their CH_3O-groups, but their penetration is not so deep (Fig. 6) to juxtapose it in the proximity of the internal proton H-5.

In the traces of the 2D ROESY maps also significant intermolecular ROEs were detected among CH_2F-protons of the enantiomers of **1** and the silyl and acetyl substituents of **2** indicating that the CH_2F (and hence the CF_3 group) must be directed towards the external surface bent at the acetyl and silyl groups. Thus, CH_2F and CF_3 groups, which protrude from the larger rim and hence are close to the acetyl groups, are also allowed to approach silylated moieties located on the smaller rim, reasonably in virtue of

the presence of *skew* glucopyranose rings and of the rotation of the glucopyranose rings about the glycosidic linkages, both leading primary groups of one unit in proximity of the secondary groups of the adjacent one (Fig. 4). In this way, the fluorinated diether **1** is allowed to give rise to attractive fluorine–silicium interactions which stabilize the two diastereoisomeric complexes (Fig. 6), but the concomitant partial inclusion of **1** from the larger rim of the cavity of **2** is allowed, in which further stabilizing hydrophobic attractive interactions occur.

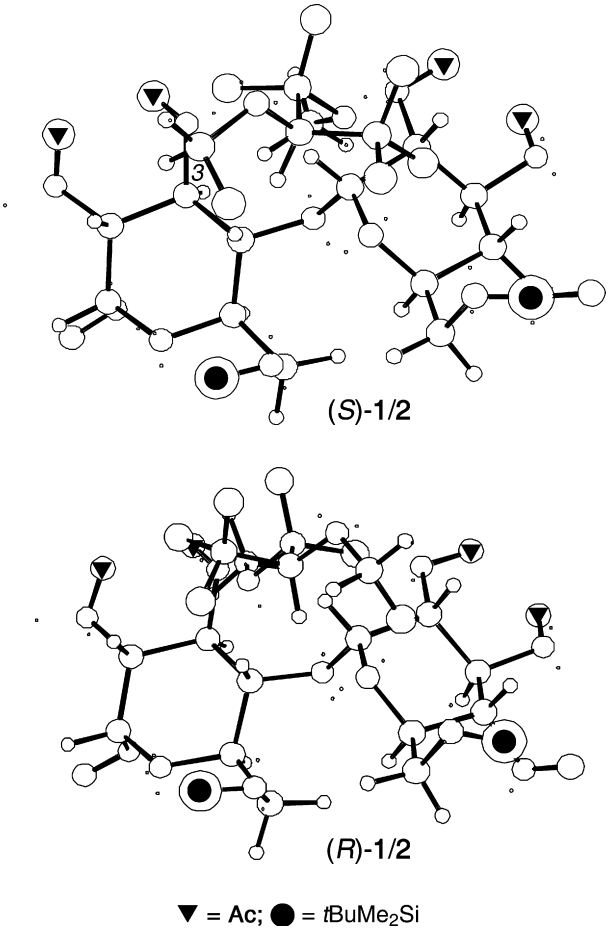

Figure 6. Schematic representation of the included enantiomers (*R*)-**1** and (*S*)-**1** close to two adjacent glucopyranose units of **2**.

3. Conclusion

The comprehension of chiral recognition processes represents a difficult task, mainly with regard to symmetrical cyclodextrins chiral selectors, the multireceptorial character of which makes difficult to point out the nature of interactions, which are responsible for enantiodiscrimination. Therefore, complementary theoretical and spectroscopic methods[28–30] have frequently been employed, among which NMR spectroscopy plays a fundamental role. As a matter of fact, several different NMR techniques can be exploited in order to investigate enantiorecognition processes to a molecular level and, more recently, the NMR measurements of diffusion coefficients have gained an increasing popularity overall in investigations involving inclusion processes.[21]

Our results demonstrated that heptakis(2,3-di-*O*-acetyl-6-*O*-*tert*-butyldimethylsilyl)-β-cyclodextrin **2**, which has been already established[7] as a powerful CSP for the gas-chromatographic separation of the two enantiomers of fluorinated compound **1**, shows a great efficiency as CSA for its enantiodiscrimination in solution by NMR spectroscopy, which confirms the great synergy existing between NMR spectroscopy and enantioselective chromatography. In spite of the fact that both the chiral analyte **1** and the chiral selector **2** are devoid of hydrogen bond donor groups (which represents a prerequisite for enantiodiscrimination by the majorities of CSAs[11–14] in solution) and the two enantiomers are included into the cyclodextrin by the same stereochemistry, unexpectedly high ^{1}H and ^{19}F non-equivalences were measured, which must be attributed to differences in the association constants of the (*S*)-**1**/**2** and (*R*)-**1**/**2** complexes. Reasonably multiple attractive fluorine–silicium interactions at the external surface of the cyclodextrin and hydrophobic attractive interactions at its internal surface, which can cooperate in virtue of the relevant deviations of the conformation of **2** from the truncated cone shape, are more efficient for (*S*)-**1** than they are for (*R*)-**1**. Such a kind of interaction mechanism is according to GC elution order and justifies the fact that both enantiomers have their proton and fluorine nuclei high frequencies shifted in the complexed forms with respect to uncomplexed one. Finally, relevant non-equivalences measured in solution strongly encourages the use of **2** as CSA for fluorinated chiral compounds, which could give an alternative to its GC use.

4. Experimental

NMR measurements were performed on spectrometers operating at 600, 150 and 282 MHz for ^{1}H, ^{13}C and ^{19}F, respectively. The temperature was controlled to ±0.1 °C. ^{1}H and ^{13}C NMR chemical shifts are referenced to TMS as an external standard. ^{19}F NMR chemical shifts are referenced to trichlorofluoromethane as external standard. The 2D NMR spectra were obtained by using standard sequences. Proton gCOSY 2D spectra were recorded in the absolute mode acquiring eight scans with a 3 s relaxation delay between acquisitions for each of 512 FIDs. The ROESY (Rotating-frame Overhauser Enhancement SpectroscopY) spectra were recorded in the phase-sensitive mode, by employing a mixing time of 0.3 s. The spectral width used was the minimum required in both dimensions. The pulse delay was maintained at 5 s; 512 hypercomplex increments of eight scans and 2K data points each were collected. The data matrix was zero-filled to 2K × 1K and a Gaussian function was applied for processing in both dimensions. Proton 1D ROESY spectra were recorded using selective pulses generated by means of the Varian Pandora Software. The selective 1D ROESY spectra were acquired with 1024 scans in 32K data points with a 10 s relaxation delay and a mixing time of 0.3 s. The gradient ^{1}H,^{13}C gHSQC spectrum was obtained in 32 scans per increment into a 2048 × 256 point data matrix. The

gradient HMBC (Heteronuclear Multiple Bond Correlation) experiment was optimized for a long-range ^{1}H–^{13}C coupling constant of 8 Hz. The spectra were acquired with 512 time increments, 32 scans per t_1 increment and a 3.5 ms delay period for suppression of one-bond correlation signals. No decoupling during acquisition was used. The selective relaxation rates were measured in the initial rate approximation by employing a selective π pulse at the selected frequency. After the delay τ, a non-selective $\pi/2$ pulse was employed to detect the longitudinal magnetization. For the biselective measurements, the two protons were inverted consecutively. Each selective relaxation rate experiment was repeated at least four times. DOSY experiments were carried out by using a stimulated echo sequence with self-compensating gradient schemes, a spectral width of 6318 Hz and 64K data points. Typically, a value of 100 ms was used for Δ, 2.0 ms for δ, and g was varied in 25 steps (16 transients each) to obtain an approximately 90–95% decrease in the resonance intensity at the largest gradient amplitudes. The baselines of all arrayed spectra were corrected prior to processing the data. After data acquisition, each FID was apodized with 1.0 Hz line broadening and Fourier transformed. The data were processed with the DOSY macro (involving the determination of the resonance heights of all the signals above a pre-established threshold and the fitting of the decay curve for each resonance to a Gaussian function) to obtain pseudo two-dimensional spectra with NMR chemical shifts along one axis and calculated diffusion coefficients along the other.

4.1. Heptakis(2,3-di-*O*-acetyl-6-*O*-*tert*-butyldimethylsilyl)-β-cyclodextrin 2

Compound **2** was synthesized according to the procedure of Takeo et al.[16] The final product was flash-chromatographed with a small amount of silica gel with toluene–ethanol (5:1, v/v) to remove non-reacted cyclodextrin and salt. After evaporation of the solvent, the residue was vacuum-dried to give slightly yellow crystals. The crude product (yield 96.5%) was used without further purification.

^{1}H NMR (600 MHz, C_6D_{12}): $\delta = 0.09$ (s, 42H; $(CH_3)_2Si$), 0.93 (s, 63H; $(CH_3)_3C$), 1.99 (s, 21H; CH_3, Ac-3), 2.01 (s, 21H; CH_3, Ac-2), 3.79 (br d, $J_{6b,6a} = 10.0$ Hz, 7H; H_{6b}), 3.88 (dd, $J_{43} = 8.6$ Hz, $J_{45} = 9.6$ Hz, 7H; H_4), 3.93 (br d, $J_{54} = 9.6$ Hz, 7H; H_5), 4.10 (br d, $J_{6a6b} = 10.0$ Hz, 7H; H_{6a}), 4.62 (dd, $J_{21} = 3.7$ Hz, $J_{23} = 9.9$ Hz, 7H; H_2), 5.23 (d, $J_{12} = 3.7$ Hz, 7H; H_1), 5.43 (dd, $J_{32} = 9.9$ Hz, $J_{34} = 8.6$ Hz, 7H; H_3); ^{13}C NMR (150 MHz, C_6D_{12}): $\delta = -5.6$ and -5.3 [$(CH_3)_2Si$], 18.2 [$(CH_3)_3C$], 20.0 (CH_3, Ac-3), 20.3 (CH_3, Ac-2), 25.7 [$(CH_3)_3C$], 62.3 (C_6), 71.5 (C_2+C_3), 72.0 (C_5), 75.6 (C_4), 96.7 (C_1), 168.9 (CO, Ac-2), 169.3 (CO, Ac-3).

Acknowledgements

The work was supported by the University of Pisa, MIUR (Project 'High performance separation systems based on chemo- and stereoselective molecular recognition' Grant 2005037725), ICCOM-CNR and 'Graduiertenkolleg—Chemie in Interphasen' of the German Research Council. The single enantiomers of compound B were kindly provided by Dr. R. Schmidt, Tübingen.

References

1. Reichle, F. M.; Conzen, P. F. *Best Pract. Res. Clin. Anaesth.* **2003**, *17*, 63–76.
2. Toscano, A.; Pancaro, C.; Giovannoni, S.; Minelli, G.; Baldi, C.; Guerrieri, G.; Crowhurst, J. A.; Peduto, V. A. *Int. J. Obstet. Anesth.* **2003**, *12*, 79–82.
3. Cunningham, D. D.; Webster, J.; Nelson, D.; Williamson, B. *J. Chromatogr., B: Anal. Technol. Biomed. Life Sci.* **1995**, *668*, 41–52.
4. Görög, S. *TrAC, Trends Anal. Chem.* **2003**, *22*, 407–415.
5. Huang, C.; Venturella, V. S.; Cholli, A. L.; Venutolo, F. M.; Silbermann, A. T.; Vernice, G. G. *J. Fluorine Chem.* **1989**, *45*, 239–253.
6. Halpern, D. *J. Fluorine Chem.* **2002**, *118*, 47–53.
7. Schmidt, R.; Roeder, M.; Oeckler, O.; Simon, A.; Schurig, V. *Chirality* **2000**, *12*, 751–755.
8. Schurig, V.; Schmidt, R. *J. Chromatogr., A* **2003**, *1000*, 311–324.
9. Schmidt, R.; Wahl, H. G.; Häberle, H.; Dieterich, H. J.; Schurig, V. *Chirality* **1999**, *11*, 206–211.
10. Grosenick, H.; Juza, M.; Schurig, V.; Klein, J. *Enantiomer* **1996**, *1*, 337–349.
11. Pirkle, W. H.; Hoover, D. J. *Top. Stereochem.* **1982**, *13*, 263–331.
12. Parker, D. *Chem. Rev.* **1991**, *91*, 1441–1457.
13. Rothchild, R. *Enantiomer* **2000**, *5*, 457–471.
14. Wenzel, T. J.; Wilcox, J. D. *Chirality* **2003**, *15*, 256–270.
15. Johnson, C. S., Jr. *Prog. Nucl. Magn. Reson. Spectrosc.* **1999**, *34*, 203–256.
16. Takeo, K.; Mitoh, H.; Uemura, K. *Carbohydr. Res.* **1989**, *187*, 203–221.
17. Grob, K. *Making and Manipulating Capillary Columns for Gas Chromatography*; Hüthig: Heidelberg, 1986.
18. Job, P. *Ann. Chim. Appl.* **1928**, *9*, 113–134.
19. Djeaini, F.; Lin, S. Z.; Perly, B.; Woussidjewe, D. *J. Pharm. Sci.* **1990**, *79*, 643–646.
20. Fielding, L. *Tetrahedron* **2000**, *56*, 6151–6170.
21. Wimmer, R.; Aachmann, F. L.; Larsen, K. L.; Peterson, S. B. *Carbohydr. Res.* **2002**, *337*, 841–849.
22. Uccello-Barretta, G.; Sicoli, G.; Balzano, F.; Salvadori, P. *Carbohydr. Res.* **2003**, *338*, 1103–1107.
23. Uccello-Barretta, G.; Sicoli, G.; Balzano, F.; Salvadori, P. *Carbohydr. Res.* **2005**, *340*, 271–281.
24. Uccello-Barretta, G.; Balzano, F.; Sicoli, G.; Scarselli, A.; Salvadori, P. *Eur. J. Org.* **2005**, 5349–5355.
25. Freeman, R.; Wittekoek, S. *J. Magn. Reson.* **1969**, *1*, 238–276.
26. *Advanced Magnetic Resonance Techniques in Systems of High Molecular Complexity*; Niccolai, N., Valensin, G., Eds.; Birkhäuser: Boston, 1986.
27. Groneborg, A. M.; Clore, G. M. *Prog. Nucl. Magn. Reson. Spectrosc.* **1985**, *17*, 1–32.
28. Dodziuk, H.; Kozminiski, W.; Ejchart, A. *Chirality* **2004**, *16*, 90–105, and references cited therein.
29. Chankvetadze, B. *Chem. Soc. Rev.* **2004**, *33*, 337–347, and references cited therein.
30. Kahle, C.; Deubner, R.; Schollmayer, C.; Scheiber, J.; Baumann, K.; Holzgrabe, U. *Eur. J. Org. Chem.* **2005**, 1578–1589.